SCA-9714

# CENTRIFUGE DATA ANALYSIS TECHNIQUES : AN SCA SURVEY ON THE CALCULATION OF DRAINAGE CAPILLARY PRESSURE CURVES FROM CENTRIFUGE MEASUREMENTS

Pierre Forbes, Institut Français du Pétrole.
at : European Commission, DGXII F-3, MO 75, Rue Montoyer 75, 1040 Brussels, Belgium.

This paper presents, on behalf of the SCA, its latest multi-lab survey on calculation of drainage capillary pressure curves from centrifuge measurements. The objective, the contributions, and analysis of the results are presented.

Fourteen contributions were received. Nineteen different solutions of the centrifuge problem were used, most of them with and without the radial correction. Data sets were interpreted close to 50 times, enough to produce a reliable statistical analysis of the error related to each solution in use (that is the error in addition to experimental error).

In practice, interpretations may differ significantly according to the solution used. The difference between interpreted curves for a given data set is comparable to the difference observed during the previous SCA study, where centrifuge capillary pressure curves were both measured and interpreted, on companion samples by different laboratories. This demonstrates that a significant part of the variation observed in that previous study was due to the use of different interpretation processes, rather than inappropriate experimental measurements.

The present survey shows that error, due the interpretation process, depends highly on the centrifuge-core geometry. For small cores (1"x1"), rotated far from the axis (Beckman L5-50P, 21.5cm), numerous solutions are accurate to within +/-3 saturation units, in addition to experimental error. For any other case (larger core or shorter radius) only a few solutions provide reliable results ; errors of 10 saturation units are not unusual for most of the other solutions. One may observe that the comparison of centrifuge curves with curves from other techniques for capillary pressure measurement (porous plate) will necessarily fail when such large errors are induced.

Most of the interpretation processes introduce a systematic negative bias on saturation. Therefore, the current approach of taking the average of results from different interpretations may lead to significant error. It is also observed that increasing the number of pressure steps, or improving the measurement accuracy below 1 to 2 saturation units, are not sufficient to improve the final accuracy.

Reliable capillary pressure curves can be obtained only by selecting one of the few appropriate solutions, including radial correction and a proper numerical implementation.

A figure is provided for the different solutions, and the different ranges of centrifuge geometry in use. It permits selection of an appropriate solution with the desire accuracy of the capillary pressure curve. Saturation error of approximately +/-3 saturation units (in addition to experimental error) may be achieved in the best cases.

## INTRODUCTION

In 1993 the Society of Core Analysts, SCA, completed a inter-laboratory survey on drainage capillary pressure measurement by centrifuge. The aim of the study was to evaluate how the different method of implementing the centrifuge technique impact the results.

Companion 1"x1" samples of Berea sandstone and Bedford Limestone were characterised, in term of porosity, grain density and permeability, and mailed world-wide to 24 laboratories for capillary pressure determination. Fifteen laboratories contributed, providing air displacing brine capillary pressure by centrifuge. Contributors included oil & gas companies, contractors and R&D institutes. Operating procedures were not specified but every laboratory was asked to provided a full description of processes and intermediate results. This was the first SCA survey on capillary pressure.

The results of that survey were analyzed and discussed during a workshop on August 9, 1993, in Houston (SCA, 1993 ; Ruth and Chen, 1995).

Significant differences between capillary pressure curves were found (Figure 1), even though the companion samples were comparable in term of porosity and permeability. The analysis focused on ways to improve and eventually standardise experimental design, measurements, and interpretation.

Many fundamental problems, concerning flow mechanisms in a centrifuge experiment, were addressed and recommendations were provided for designing centrifuge experiments. However, it was impossible to isolate the source of the variability, whether is was from measurements or from interpretation processes.

Indeed, in the centrifuge method, the capillary pressure curve is not directly measured, but is calculated, from fluid production measurements, using various approximate methods. During the SCA 1993 workshop, these methods were also discussed (Forbes, 1993). It appeared that the choice of the calculation procedure may potentially affect the resultant capillary pressure curve. Accordingly, it was decided to launch a second survey specific to the evaluation of the calculation methods for drainage centrifuge capillary pressure curves. That calculation survey is presented below.

## I THE CENTRIFUGE TECHNIQUE

The centrifuge technique, for capillary pressure measurement on core samples, was introduced by Hassler and Brunner (1945) and Slobod et al. (1951). It requires two steps, the measurement of the centrifuge fluid production data and transformation of that data into capillary pressure curves. Various procedures may be used for both steps and, as previously stated, this paper addresses the second step only, that is the processes of interpretation. Discussions of the physical assumptions and measurement procedures are available in Hirasaki et al. (1988), Hirasaki and Rohan (1993) and O'Meara et al. (1988, 1992).

During the past decades, advances have been made in many aspects of centrifuge data processing. However, one has to keep in mind that it has not been perfected. Numerous publications claimed to provide improved solutions while later being corrected, and sometimes contradicted, (see for instance Hoffman, 1963 and then Luffel, 1964, or, van Domselaar, 1984 and then Ayappa et al., 1989, or, Rajan, 1986 and then Ayappa et al., 1989, or, Christiansen, 1992 and Forbes et al., 1994a, ...). Indeed, a number of different interpretation techniques are in used in the industry. Which ones are reliable ?

The centrifuge technique consists of rotating a core at various angular velocities, ω, (Figure. 2). The core contains two fluids for which capillary pressure is to be determined. In the drainage process, the denser fluid is forced out of the core by rotation. Fluid production, or average fluid saturation in the core, is measured at hydrostatic equilibrium for every rotation speed.

The capillary pressure curve can be deduced from the measurements, if the related inversion integral problem can be solved.

Since Hassler and Brunner (1945), different formulations of that integral problem have been proposed. The main assumptions are that hydrostatic equilibrium is actually reached for each measurement step, and that the capillary pressure is zero where the fluid is flowing out of the core (boundary condition).

For a given angular velocities ω, the pressure field within the sample is written $Pc_{(r,Z)}$, the capillary pressure curve S(Pc) and the measured average saturation, <S>. <S> is linked to S(Pc) by :

$$\langle S \rangle = \frac{1}{L \pi R^2} \int_{core} S_{(Pc(r,Z))} dv \quad (1)$$

*L is the core plug length, R is the radius of core, r is the rotation radius, Z is the vertical coordinate, dv is the elementary volume (Figure 2).*

$Pc_{(r,Z)}$, can be determined locally within the core. Forbes, (1997a, that meeting), shows how $Pc_{(r,Z)}$ varies inside the core and how the integral of equation (1) can be reworked and normalized into :

$$<S>_{B,N,M} = \frac{1+\sqrt{1-B}}{2}\int_{X=0}^{X=1}\frac{dx}{\sqrt{1-Bx}}\int_{y=0}^{y=1}\frac{2}{\Pi}\sqrt{\frac{y}{1-y}}dy\int_{Z=-1}^{Z=1}\frac{dz}{2}S_{[P_1(X+Ny+2NM\sqrt{y}+Nn)]} \qquad (2)$$

with :

$$B=1-(\frac{r_1}{r_3})^2, \quad N=\frac{R^2}{r_3^2-r_1^2}, \quad M=\frac{g}{\omega^2 R}, \quad P_1=\frac{1}{2}\Delta\rho\omega^2(r_3^2-r_1^2) \qquad (3)$$

and

n=2M-1 if M>1 or $n=M^2$ if M<1

For a set of discrete measurements {<S>; ω}, or {<S>; $P_1$}, the general **"centrifuge problem"** consist of retrieving S(Pc) by inverting the equation (1) that is : $<S>(P_1) = <S>_{B,N,M}(P_1)$ **(4)**

## II THE METHODS IN USE.

There are numerous methods to solve the centrifuge problem. All methods involve both a solution for equation (4) and a numerical implementation scheme for that solution. Indeed, none of the solutions in use addresses the complete equation (4), only simplified forms of it. The solutions are labelled hereafter by acronyms (HB, HOF,....), defined in the following sections and used subsequently when referring to these solutions.

### *II. 1 The Hassler and Brunner solution, HB*

The very first Hassler and Brunner solution (Hassler and Brunner, 1945) is the simplest, but the poorest, solution of the saturation equation. Its use requires the assumptions B=0, N=0 and M=0. That is $<S>(P_1) = <S>_{0,0,0}(P_1)$,

$$or \; <S> = \int_{X=0}^{X=1} dx S_{[PX]} \qquad (5) \qquad \text{which is inverted as} \qquad S_{HB}(P) = <S>(P) + P\frac{d<S>}{dP}(P) \qquad (6)$$

This solution is denoted $S_{HB}$. It is assumed that the pressure field in the core is linear, (neither radial nor centrifugal), and the gravity is neglected. These assumptions can be satisfied for very short and narrow samples spun far from the rotation axis. As demonstrated by Forbes (1991, 1994), this solution is always significantly lower, in term of saturation, than the true S(Pc) solution. This is because B is usually far from zero. Large errors may be expected when it is used for high B or N values.

### *II. 2 The other solutions in use in the Industry.*

Most of the other solutions address the centrifuge equation while neglecting radial (N=0) and gravity (M=0) effects. That is $<S>(P_1) = <S>_{B,0,0}(P_1)$ or :

$$<S>_{(P_1)} = \frac{(1+\sqrt{1-B})}{2}\int_{X=0}^{X=1}\frac{S_{(xP_1)}}{\sqrt{1-Bx}}dx \qquad (7)$$

$$or\ S_{(P_1)} = \frac{2\sqrt{1-B}}{(1+\sqrt{1-B})} \frac{dP<S>}{dP}(P_1) + \int_{X=0}^{X=1} S_{(xP_1)} \frac{Bx}{1-Bx} \frac{\sqrt{1-B}}{2\sqrt{1-Bx}} dx \qquad \textbf{(8)}$$

These solutions are as follows :

***a) The Hassler and Brunner second solution, HB2***, Hassler and Brunner, 1945 ; Hermansen et al., 1991.

$$S_{HB2}(P_1) = S_1(P_1) + S_2(P_1) + S_3(P_1) + \ldots\ldots S_n(P_1) + \ldots\ldots \ with$$
$$S_1(P_1) = S_{HB}(P_1) \quad and \quad S_{n+1}(P_1) = \frac{d}{dP}\left(P_1 \int_{X=0}^{X=1} \left(1 - \frac{1+\sqrt{1-B}}{2\sqrt{1-Bx}}\right) S_n(xP_1)\, dx\right) \qquad \textbf{(9)}$$
$$or \quad S_{n+1}(P_1) = -\frac{1-\sqrt{1-B}}{2\sqrt{1-B}} S_n(P_1) + \frac{(1+\sqrt{1-B})B}{4} \int_{X=0}^{X=1} \frac{x}{(1-Bx)^{3/2}} S_n(xP_1)\, dx$$

***b) The van Domselaar solution, DOM***, van Domselaar, 1984

$$S_{DOM}(P_1) = <S>(P_1) + \frac{2\sqrt{1-B}}{1+\sqrt{1-B}} P_1 \frac{d<S>}{dP}(P_1) \qquad \textbf{(10)}$$

***c) The Hoffman solution, HOF,*** Hoffman, 1963

$$S_{HOF}(P_1) = \frac{2\sqrt{1-B}}{1+\sqrt{1-B}} S_{HB}(P_1) \qquad \textbf{(11)}$$

***d) The Rajan solution, RJ,*** Rajan, 1986

$$S_{RJ}(P_1) = S_{DOM}(P_1) + \frac{\sqrt{1-B}}{B} P_1 \int_{X=0}^{X=1} \left(\frac{1-\sqrt{1-Bx}}{\sqrt{1-Bx}}\right)^2 \frac{d<S>}{dP}(xP_1)\, dx \qquad \textbf{(12)}$$

***e) The Forbes first solution***, ***S***$\alpha$, Forbes, 1991, 1994

$$S_{\alpha}(P_1) = <S>(P_1) + \frac{1}{1+\alpha} P_1 \frac{d<S>}{dP}(P_1), \qquad with \quad \alpha = \frac{1-\sqrt{1-B}}{1+2\sqrt{1-B}} \qquad \textbf{(13)}$$

***f) The Clinch approximate solution, CAP***, Clinch, 1995

Clinch considered that the pressure and saturation profiles in the core, at rotation speed $\omega_{i-1}$ (average saturation $<S>_{i-1}$ and inlet pressure $P_{i-1}$), can be scaled to describe the part of the profiles at $\omega_i$ for which P is lower than $P_{i-1}$. Balance with the average saturation and inlet pressure at $\omega_i$ permits calculation of the mean local saturation, $Se_i$, and pressure, $Pe_i$, in the remaining part of the core ($P_{i-1}<P<P_i$). Clinch averaged ($Se_i$, $Pe_i$), with the HB and DOM solutions in order to propose the CAP solution. It can be rearranged in a form close to the S$\alpha$ formulation, with $\alpha$ being pressure dependent :

$$S_{(p_i)} = \langle S \rangle_i + a \frac{\Delta \langle S \rangle}{\Delta P} P_i, \text{ with } a = \left(1 + \frac{B}{2} \frac{1-\sqrt{1-B}}{2\sqrt{1-B}}\right) \frac{P_{i-1}}{P_i} \frac{\sqrt{1-B} + \sqrt{1 - B\frac{P_{i-1}}{P_i}}}{1 + \sqrt{1 - B\frac{P_{i-1}}{P_i}}}$$

$$\frac{\Delta \langle S \rangle}{\Delta P} = \frac{\langle S \rangle_{i-1} - \langle S \rangle_i}{P_{i-1} - P_i}, \; p_i = P_i + \frac{P_{i-1} - P_i}{6} \frac{2\sqrt{1-B} + \sqrt{1 - B\frac{P_{i-1}}{P_i}}}{\sqrt{1-B} + \sqrt{1 - B\frac{P_{i-1}}{P_i}}} \qquad \textbf{(14)}$$

***g) The Chen and Ruth solution, CRM***, Chen and Ruth, 1993

This method uses the Sα formulation above, but the α value is optimized by fitting numerically the integral (7) to the <S> experimental data, when S is taken as Sα. The fitted α value is always very close to the value given by equation (13). In the survey, this method is not distinguishable from the S α one.

***h) The Forbes second solution, S***αβ, Forbes, 1991, 1994

$$S_{\alpha\beta} = \frac{B}{2} S_\beta + \left(1 - \frac{B}{2}\right) S_\alpha \quad \text{with } S_\beta(P_1) = (1+\beta) \int_{x=0}^{x=1} x^\beta S_{HB}(xP_1)\, dx, \text{ and } \beta = 2\frac{1+2\sqrt{1-B}}{1-\sqrt{1-B}} \qquad \textbf{(15)}$$

***i) The Ruth and Wong first solution, RW1***, Ruth and Wong 1988, 1991 ; Melrose, 1988

The method uses a linear interpolation of S(P) on every segment $\{P_{i-1}, P_i\}$, where $P_i$ are the experimental values of $P_1$. S(P) linear variation is replaced in the integral of equation (8), segmented in $\{P_0, P_1\}$, $\{P_1, P_2\}$, ...., or replaced in an approximation of that integral derived by Melrose, 1988. $S_i$ is then deduced sequentially from the experimental data and preceding values of S (Ruth and Wong 1988) as :

$$S_i = \frac{2\sqrt{1-B}}{(1+\sqrt{1-B})} \frac{d\langle S \rangle}{dP}(P_i)\; G(P_{i-1}, \langle S \rangle_{i-1}, S_{i-1}, \ldots) + F(P_{i-1}, \langle S \rangle_{i-1}, S_{i-1}, \ldots) \qquad \textbf{(16)}$$

***j) The Ruth and Wong second solution, RW2,*** Ruth and Wong 1990

As RW1, the method, also called Experimental Integral Method, uses a linear interpolation of S(P) in segment $\{P_{i-1}, P_i\}$. Here, the linear variation of S is replaced directly in equation (7), segmented and integrated numerically or analytically. This leads again to a sequential determination of $S_i$ from the experimental data and preceding values of S (see Ruth and Wong 1990).

***k) The Hermansen solution, HER***, Hermansen et al., 1991

The method is similar to RW1 or RW2. Instead of being assumed to vary linearly on segment $\{P_{i-1}, P_i\}$, S is assumed to be constant and equal to $S_{i-1/2} = S((P_{i-1}+P_i)/2)$, (modified midpoint method, Andersen and White, 1971). $S_{i-1/2}$ is then deduced sequentially as an analytical expression of the experimental data and preceding values of S (Hermansen et al., 1991) as :

$$S_{n-\frac{1}{2}} = \frac{(1-\sqrt{1-B})\langle S_n \rangle - \sum_1^{n-1} S_{i-\frac{1}{2}}(U_{n,i-1} - U_{n,i})}{U_{n.n-1} - U_{n.n}}, \quad \text{with } U_{n,i} = \sqrt{1 - B\frac{P_i}{P_n}} \qquad \textbf{(17)}$$

Scattering in the results is prevented by smoothing, replacing $S_{n-1/2}$ by 1/4 ($S_{n-3/2} + 2S_{n-1/2} + S_{n+1/2}$).

***l) The Parameter Estimation solutions***, Bentsen and Anli, 1977, Golaz and Bentsen, 1980

The "parameter estimation methods" assume a parametric function for the capillary pressure curve. This function usually depends on three to four parameters which are optimized by fitting the integral (7) to the experimental data. It requires repetitive numerical integration of equation (7). Parametric functions in use are (Anli, 1973 ; Bentsen and Anli, 1977 ; Golaz and Bentsen, 1980 ; Corey, 1954 ; Thomeer, 1960 ; Glotin et al., 1991 ; Chen at al, 1992 ; van Domselaar, 1984 ; Forbes, 1993 ; Hirasaki and Rohan, 1993):

$$Pc=\sigma\left(\frac{1-S}{S-S_{ir}}\right)^{n}+P_d;\quad Pc=\sigma\ln\left(\frac{S-S_{ir}}{1-S_{ir}}\right)+P_d;\quad Pc=P_d+\sigma(1-S)^{n},\ for\ S>S_{ir};$$
$$Pc=P_d\ EXP\left(\frac{-F}{\ln\left(\frac{1-S}{1-S_{ir}}\right)}\right);\quad \frac{S-S_{ir}}{1-S_{ir}}=\sum_i\sigma_i\left(\frac{Pc}{P_d}\right)^{i};\qquad \textbf{(18)}$$
$$\frac{S-S_{ir}}{1-S_{ir}}=\left(\frac{P_d}{Pc}\right)^{n};\quad \frac{S-S_{ir}}{1-S_{ir}}=\ln\left(1+\sigma\frac{P_d}{Pc}\right);\quad \frac{S-S_{ir}}{1-S_{ir}}=\frac{1}{1+\sigma(Pc-P_d)^{n}}$$

The three first were used in that survey. Related solutions are referred as ***PAR*** : optimisation of σ, Sir, n and Pd in the first relationship ; ***B11*** : optimisation of σ and Pd in the second relationship (Sir being imposed by the user) ; ***B12*** : optimisation of σ, Sir and Pd in the second relationship; ***B21*** : optimisation of σ, n and Pd in the third relationship; ***B22*** : optimisation of σ, Sir, n and Pd in the third relationship.

***m) The Spline and B-spline solution, SPL,*** Nordtvedt, 1989 ; Nordtvedt et al., 1990 ; Nordtvedt and Kolltveit, 1991 ; Kolltveit et al., 1996.

The parameter estimation methods reported above are usually related to functions which are too simplistic to described the shape of capillary pressure curves. A proper way to deal with that description is to use splines or B-spline description, i.e. piecewise polynomials functions of order 2 or 3 in practice (Nordtvedt, 1989, Nordtvedt et al., 1990). Fitting the spline parameters to the observed data <S> through equation (7) requires a sophisticated algorithm. However the optimization procedure may be simplified because equation (7) can be solved analytically for a polynomial expression of S, i.e. for splines. A linear system of equations is obtained from equation (7). In addition, the SPL method can be operated including a regularization process to prevent oscillation in the solution (Kolltveit et al., 1996).

***o) The Center of Force solution,COF***, Jaimes, 1991,

The method is based on the assumption that the average saturation in the rotating core is the same that the local saturation at the location of the Center of Forces, i.e. where an unique total force will produce the same movement as the set of forces acting over the different parts of the core liquid. At that Center, the saturation is assumed to be the measured average saturation, S=<S>, and the method consists of evaluating the local capillary pressure at that location (Jaimes, 1991). This method is unique, because it is the only one involving pressure evaluation as opposed to saturation evaluation.

***n) The Skuse solution, SK,*** Skuse et al., 1988, (not used it that survey)

$$S_{SK}(P_1)=S_{HOF}(P_1)+\frac{\sqrt{1-B}}{2B}P_1\int_{x=0}^{x=1}\frac{x}{(1-Bx)^{\frac{3}{2}}}\frac{dP<S>}{dP}(xP_1)\,dx\qquad \textbf{(19)}$$

That solution is quite close to the Rajan solution.

***p) The Sν solution***, Forbes, 1991, (not used it that survey)

That solution is convenient for calculating directly a corrected USBM wettability index (Hirasaki et al., 1990 ; Donaldson et al., 1969 ; Anderson, 1986). It is given as :

$$S_\nu(P_1)=\frac{\sin(\pi\nu)}{(1-\nu)\pi}\frac{d}{dP}\left[P_1\int_{x=0}^{x=1}\left(\frac{x}{1-x}\right)^{1-\nu}\langle S\rangle(xP_1)dx\right],\ with\ \ \nu=\frac{1-\sqrt{1-B}}{2+\sqrt{1-B}} \qquad \textbf{(20)}$$

***q) Direct solutions***, King et al., 1986, 1990 , Forbes, 1993, (not used it that survey)

An exact direct solution consists of analytically inverting equation (7) by the use of a complementary weight function, which is pre-defined and not dependent on the capillary pressure curve. Solutions are on the form as the one proposed by Forbes, 1993 :

$$S(P_1)=S_{HOF}(P_1)+\frac{d}{dP}\left[P_1\int_{x=0}^{x=1}F_B(x)\langle S\rangle(xP_1)dx\right],\ \ with$$
$$F_B\ defined\ by\ \int_{x=y}^{x=1}F_B(x)\left(\sqrt{1-B\frac{y}{x}}-\sqrt{1-B}\right)dx=\frac{(\sqrt{1-By}-\sqrt{1-B})^2}{(1+\sqrt{1-B})} \qquad \textbf{(21)}$$

***II. 3 The use of constraints and proper algorithms.***

Implementation of the previous solutions requires the use of different algorithms and numerical schemes. The results from a given solution can vary significantly depending on the implementation scheme used (see below).

***a) Algorithms and calculation schemes***

Algorithms are required for calculating integrals and derivatives or for sequential determinations. A study of differencing schemes, can be found in Ruth and Wong, 1990.

Calculating Sα for instance can be done using one of the following expressions or their combination:

$$S_\alpha=\langle S\rangle+\frac{1}{1+\alpha}P\frac{d\langle S\rangle}{dP}=\frac{dP^{1+\alpha}\langle S\rangle}{dP^{1+\alpha}}=\frac{\alpha}{1+\alpha}\langle S\rangle+\frac{1}{1+\alpha}\frac{dP\langle S\rangle}{dP}=\frac{1}{(1+\alpha)P^\alpha}\frac{dP^{1+\alpha}\langle S\rangle}{dP} \qquad \textbf{(22)}$$

Backward, central, forward differencing, or a least squares differencing scheme, or curve fitting can be used with each of them. Therefore, even this simple calculation can be implemented in more than 20 different ways and much more by combination (central differencing on the second form provides the best results).

***b) Consistency constraints***

All the previous solutions utilize equation (7), the measurement $\langle S\rangle(P_1)$ being supposed to be the simple integral $\langle S\rangle_{B,0,0}(P_1)$. A number of constraints can be derived from $\langle S\rangle(P_1)=\langle S\rangle_{B,0,0}(P_1)$, (Forbes, 1991). They rely on the variation of S, <S> or Pd, the threshold pressure. They can be used to correct S or <S>, compensating partly for the approximate nature of equation (7) or for the experimental error in the <S> measurements. Therefore, using such constraints potentially improves the determination of the capillary pressure curve (see below). For instance, the following should be tested according to equation (7):

$$S_{(P_1)} \text{ decreasing and } S_{(P_1)} \le \langle S\rangle(P_1) - \frac{1-\sqrt{1-B\frac{P_d}{P_1}}}{\sqrt{1-B\frac{P_d}{P_1}}-\sqrt{1-B}}\left(S_d-\langle S\rangle(P_1)\right)$$

$$P_d \le P_1\left(\frac{\langle S\rangle(P_1)}{S_d}\right)^{\frac{2\sqrt{1-B}}{1+\sqrt{1-B}}}, \text{ or } P_d \le P_1\left(\frac{\langle S\rangle(P_1)}{S_d}\right)^{\frac{2-(1-\sqrt{1-B})\left(\frac{\langle S\rangle(P_1)}{S_d}\right)}{1+\sqrt{1-B}}} \qquad \textbf{(23)}$$

$$P_1^{\frac{1+\sqrt{1-B}}{2\sqrt{1-B}}}\langle S\rangle(P_1) \text{ increasing, } \left(S_d-\langle S\rangle(P_1)\right)\frac{1-\sqrt{1-B}}{\sqrt{1-B\frac{P_d}{P_1}}-\sqrt{1-B}} \text{ increasing}$$

The way of these constraints are implemented, or not, may change the interpretation and is one characteristic of the calculation method. *In this paper, methods including these consistency constraints are labelled with "C".*

***II. 4 The radial and gravity corrections.*** (Forbes et al. 1994 ; Forbes and Fleury, 1995 ; Forbes 1997a).

The impact of neglecting radial effects (N=0) and gravity effects (M=0) in equation (4) has been pointed out in the recent past by (Christiansen and Cerise, 1987 ; Blackwell, 1991 ; Ayappa et al., 1994 ; Christiansen, 1992 ; Chen and Ruth, 1994 ; Forbes et al., 1994a ; Forbes and Fleury, 1995 ; Fleury and Forbes, 1995 ; Forbes, 1997a). Forbes et al. 1994b, and Forbes, 1997a, proposed a correction to account for these effects. It consists of replacing the experimental data $\{P_1 ; \langle S\rangle[P_1]\}$ by $\{P_1/b; \langle S\rangle[P_1]+a_o(\langle S\rangle[a_oP_1]-\langle S\rangle[P_1])\}$, before processing any of the above solutions, according to :

| ao | bo | C | 1/b - 1/bo |
|---|---|---|---|
| $\frac{3/4N\,(1+(1-B)^{1/2})}{2(1+N)}$ | $\frac{1+0.23N/(1+N)}{(1+N)}$ | $\frac{N\,(4+2(1-B)^{1/2})}{(5+(1-B)^{1/2})}$ | M>1 : (4M-1.75) C<br>0<M<1 : $2.25M^{1.7}$ C |

When gravity is neglected, M reduces to 0, and b to bo, that is to the "radial correction".

The effect of gravity may be significant at low rotation speed only (Forbes, 1997a). In practice however, for the capillary pressure cases used in this survey, gravity has an effect far below the experimental error. Only radial correction may have a significant impact.

*Methods including the radial correction are labelled with "R".*

## III THE CALCULATION SURVEY

The main purpose of the survey was to determine how centrifuge data analysis techniques affect the accuracy of the derived capillary pressure curves. To achieve this goal, artificial centrifuge data were calculated, for given capillary pressure curves, and provided for interpretation.

An additional objective was to provide a data-base of synthetic centrifuge measurements, covering the range of centrifuge and core geometries encountered in centrifuge experiments, that can be used to test any interpretation method that might be developed in the future. The initial "true" capillary pressure curves and centrifuge/core geometries, to be used in the survey, were selected by reviewing the experimental conditions reported in the literature (see Forbes, 1997b).

Actual core diameter and length usually fall in the range 2.5-5 cm (1" to 2") and 1.3-7.6 cm. respectively. Core are located between 6 cm and 24.3 cm from the rotation axis (external radius). Their

porosity is generally about 10 to 25%. Fluid density is close to 1 kg/l for the brine, 0.8 kg/l for oil and very low for gas.

Rotation speeds range from 150 RPM to 8000 RPM and the related error of measurement on the best centrifuges is at least 10 RPM. The error on production volume measurements is at least in the range of 0.02 to 0.1 cc, (usually leading to 1 to 2 saturation units of uncertainty on the average saturation determination).

Measurements are generally performed for 5 to 24 rotation steps (see for instance Ward and Morrow, 1985 ; Melrose, 1990 ; SCA 93).

### *III 1 The selected "true" capillary pressure curves*

The shapes of the selected curves may present one or two curvatures (bump), sharp bending, pressure threshold, or a flat and regular behaviour in the high saturation range (Figure 4). All these shapes can be found in the literature, including the bumped or so-called double porosity curves (case 4 see Christiansen, 1992 and its figure 4 ; Case 9, see Sabatier, 1994 or Nordtvedt et al., 1990 ; Case 10, see Ayappa et al., 1989 or Bentsen and Anli, 1977).

Pressure ranges from few psi to more than 200 psi as reported in the current literature (see Forbes, 1997b).

Ten artificial centrifuge experiments were constructed by combining various capillary pressure curves and centrifuge/core geometries (Figure 4). They were chosen to cover most of the situations encountered in drainage capillary pressure measurement by centrifuging. They therefore do not focus only on the most frequent situations. Figure 3 shows the distribution of B and N parameters for these 10 cases. Cases 6-9 cover the situation of short radius (8.6 cm.) centrifuges, cases 2-3 are related to intermediate radius (9.38 cm.), cases 7-8-10 to long radius geometry and cases 1-5 to flat core geometry. The Figure 3 also shows how the cases can be grouped to permit a statistical analysis on the whole range of the B, N diagram.

Only 10 cases were selected, in order to limit the extent of the survey to what should be "feasible" in a short time for most petrophysical laboratories.

### *III 2 Generation of artificial data*

For each of the 10 cases, selected capillary pressure curves have been taken as parametric functions, combinations of the last three relationships of equation (17), (Forbes, 1997b). The average saturation curve $\langle S \rangle_{B, N, M} (P_1)$ has been calculated using the full integral (2). A sampling $\{\langle S \rangle_{B, N, M} ; P_1\}$, on that curve, was then transformed in production volume, V, and rotation speed, $\omega$, according to the selected centrifuge geometry and core characteristics (Figure 4). Random error have been introduced, within the range given for each case (Figure 4), finally leading to sets of artificial centrifuge data $\{V ; \omega\}$.

Figure 4 shows the different $\langle S \rangle_{B,N,M}(P_1)$ curves and the corresponding artificial data set for cases 1 to 10 (black dots). The difference between $\langle S \rangle_{B, N, M} (P_1)$ and the black dots represents the experimental error.

The 10 artificial centrifuge data sets and the related centrifuge / core characteristics were provided to laboratories for transformation into capillary pressure curves, S(P). The true S(Pc) curves were not provided.

### *III 3 Contributions*

Fourteen contributions from oil and gas companies, core analysis contractors and R&D institutes were provided. Most laboratories used several methods, providing in total 45 to 50 different processings of each of the 10 data sets. 19 of the previously discussed solutions were used, with and without radial correction, providing at least 39 distinctive methods of data interpretation.

Every result consists of a set of values $\{S_i, P_i\}$, the interpreted capillary pressure curve S(Pc), and some explanation on the corresponding interpretation method (Forbes, 1997b).

For any interpretation $\{S_i, P_i\}$, one measures the departure from the true S(Pc), by $S_i - S(P_i)$. If $S_i - S(P_i)$ is within the experimental error +/-?<S> (as introduced in the corresponding centrifuge data set), the processing is not generating any additional error (above experimental error). If $S_i - S(P_i)$ is higher than +?<S>, or lower than -?<S>, the processing induces a positive or negative additional error.

For a full set $\{S_i, P_i\}$, or for a group of sets, one defines L, W and H as the fractions of the group for which $S_i - S(P_i)$ is respectively lower, within or higher than the initial experimental error (L+W+H= 1). W is the fraction of undamaged result, i.e. those for which no additional error has been added by the processing. IF L>H, a negative bias has been introduced, while if H>L a positive bias has been introduced.

For additional quantitative evaluation of the efficiency of the interpretation methods, one also introduces $?_{90}^-$ and $?_{90}^+$. For a full set $\{S_i, P_i\}$, or for a group of sets, $[-?_{90}^- ; ?_{90}^+]$ is defined as the shorter interval containing 90% of additional errors due to the processing. That is that 90% of the $\{S_i, P_i\}$ are within $[-?_{90}^- - ?<S> ;??_{90}^+ + ?<S>]$ around the true S(Pc) curve. $[-?_{90}^- ; ?_{90}^+]$ is a measure of the additional error bar due to the interpretation method used. The lower $[-?_{90}^- ; ?_{90}^+]$ is, the more accurate the method is. If $?_{90}^+ >>?_{90}^-$, or $?_{90}^- >>?_{90}^+$, a positive, or respectively negative, bias is introduced.

In the analyses below, different grouping of $\{S_i ; P_i\}$ sets are considered. Contributions have been gathered by case (#1 to 10), then gathered by interpretation method and finally gathered by solution used.

### *III 4 Analysis by case*

Figures 5 and 6 show the interpreted capillary pressure sets $\{S_i, P_i\}$ for cases 2 and 7. Case 7 is one of the best, i.e. with a low spreading of the different contributions around the true curve, S(Pc), (+/- 5 saturation units). Case 2 is one of the worst, with a very large spreading. The accuracy of most of the method in use is questionable, especially if one considers that case 2 is related to a very common capillary pressure curve and was reasonably well defined by 10 rotation steps of measurement and a low saturation error, ?<S>=0.007 (frac.).

In general the present spreading (Figure 6) is quite comparable to the dispersion reported in the previous centrifuge SCA experimental survey on companion samples (Figure 1, SCA, 1993). This suggests that interpretation processes alone can account for the inaccuracy in centrifuge capillary pressure determination. One might therefore question how relevant the comparisons between centrifuge Pc curves and Pc curves obtained by other techniques (porous plate, mercury injection, ...) are, even when centrifuge experimental measurements were carefully done.

The reason cases have a large dispersion, such as case 2, is a centrifuge/core geometry leading to high value for the B or N parameters. On the other hand, cases with low B and N values, such as cases 9 or 10, have been properly retrieved, even with more "exotic" shapes and higher measurement error, ?<S>=0.02 (frac.). This suggests that parameters B, N are mainly controlling the inaccuracy of interpretation methods, while the curve shape or the experimental accuracy have lesser effect.

The variation of W versus N and B is shown in Figure 7. For cases with N>0.04 or B>0.7 less than one third of the saturation determinations (gathering all the contributions) is kept within the experimental error range (W<30%). Figure 8 shows that increasing the number of measurement steps, nb, is not sufficient to increase the accuracy of the interpretation unless 15 to 25 steps are performed.

Figure 9 shows the W changes versus the measurement error, ?<S>, attributed to the different cases. Reducing the measurement error below 2 saturation units is also not sufficient to increase W, i.e. to reduce the inaccuracy introduced by neglecting the centrifuge / core geometry.

To conclude, the centrifuge and core geometry appears to be the main source of error for most of the interpretation methods in used. The choice of the method, according to B and N values, appears to be of prime importance, much more than improving experimental conditions (i.e. accuracy of production measurement or number of rotation step). This is especially critical when B>0.7 or N>0.04, and includes the most common geometry of 1"x1" sample run at 8.6 cm from the centrifuge axis.

***III 5 Analysis by methods (individual contributions)***

As discussed previously, a given solution, Sα for instance, may be implemented using a number of different schemes and an interpretation method consists of both the solution and its numerical implementation. Therefore, each individual contribution may be considered as a distinct method, even when using the same solution (implementations are potentially different from a laboratory to another one). Consequently L, H, W, $\delta_{90}^-$ or $\delta_{90}^+$ may show different values for two different implementations of the same solution.

The effect of the numerical implementation scheme used is shown in Figure 10. Figure 10 is an LWH ternary diagram for those of the solutions provided by at least two different contributors (Sαβ and SαβR are not plotted because the same numerical implementation was used by the contributors). It illustrates clearly that the way a given solution is applied, may significantly affect its accuracy. For the HB solution, one obtains less than 10 % to more than 30% of undamaged results (W) depending on the way it has been applied. A similar analysis, using $\delta_{90}^-$ and $\delta_{90}^+$, shows a difference of 2 to 8 saturation units in the additional error due to the data processing when different implementations are used (Forbes, 1997b).

The readily conclusion is that the choice of an optimal numerical implementation for a given "solution" may significantly improve the capillary pressure curve determination.

***III 6 Analysis by solutions***

When analyzing the results by solutions (HB, HB2, .....) and calculating L, W, H, one can determine the accuracy of these solutions (as an average over the different implementations provided). The solutions with and without radial correction are plotted separately on Figure 11. Arrows indicate the effect of the radial correction. Additionally Sα and SαR solutions are shown including, or not, consistency constraints as indicated by the arrow "C" (Figure 11). The zones of negative or positive bias are indicated.

Using the HB or HOF solutions, or neglecting radial effect, introduces a systematic negative bias (L>>H, see also Forbes, 1991 for $S_{HB}$<S and Forbes et al., 1994 for the impact of radial effect). The van Domselaar (DOM) and the Clinch (CAP) solutions are the only ones leading to better accuracy if not corrected for radial effect, because of compensating errors (negative bias of neglecting radial effect and systematic positive bias of the solution itself, S<$S_{DOM}$, see Forbes, 1991). Such a compensation is effective on average, over the 10 cases of the survey. For individual case, it is however not relevant, depending on the extend of radial effect. The CAP solution in fact includes partly the DOM solution. Both generate positive bias when corrected for radial effect (Figures 11, 12). Because of this, the use of the DOM or CAP solutions is not recommended.

Because most of the solutions introduce a negative bias (L>H, Figure 11), especially if not corrected for radial effect, the common practice of using different solutions and averaging the results is totally irrelevant. Errors being dominantly negative, no compensation is achieved by averaging.

Quantitatively, one can note (arrows on Figure 11) that using radial correction or consistency constraints increase by about 10 units the fraction of undamaged results (W). It reduces the additional error interval, [$-\delta_{90}^-$ ; $\delta_{90}^+$], by 2 to 9 saturation units.

The most appropriate solutions, over the whole set of 10 artificial cases, are therefore those located in the top of the LWH diagram. They are SPLR, Sαβ(c), SαβR(c), SαR(c) and all require radial correction or consistency constraints.

**IV APPLICATION or "How to use the survey results"**

As stated previously, the geometry of the centrifuge measurement (B,N) mainly controls the accuracy of the inversion processes in use (Figures 7, 8, 9). The behaviour of a given solution may therefore depend on these geometry parameters. The previous behaviour analysis gathering all the cases #1 to 10, for every solution, needs to be refined according to B and N values.

For every solution (HB, HB2,.....), $\delta_{90}^-$ and $\delta_{90}^+$ have been calculated on sub-group of cases (part of #1 to 10) as described on Figure 3. Gathering interpretations of cases 2, 4 and 7, for instance, will demonstrate the behaviour of the solutions for the range B>0.7, N<0.025. Gathering results for cases 6 and 9 refers to N≈0.04, B<0.7.....(see Figure 3).

Figure 12 shows intervals $[-\delta_{90}^+ ; \delta_{90}^-]$ as function of B, N and the solution used.$[-\delta_{90}^+ ; \delta_{90}^-]$ which may be considered as the error bar on saturation determination due to the interpretation of centrifuge data using the related solution. This is the bar to be fixed on the interpretation dots, (Si ; Pi), to get the zone where the exact capillary pressure curve is (at 90%).

On may use Figure 12 either to evaluate the error in the capillary pressure curve when a given solution is used, or to select an appropriate solution to be used in order to achieve a desired accuracy in the results. The total error in saturation determination is therefore the error due to processing, as provided by Figure 12, plus the initial experimental error in average saturation measurements (usually in the range of 1 to 2 saturation units).

For long radius geometry (21.5cm) and 1"x1" core, one may expect to obtain the capillary pressure curve with an additional error of +/- 1 to 3 saturation units for number of the solutions in use (Figure 12). However for any other geometry much higher errors are associated to most of the solutions. Only few, over the 36 displayed on Figure 12, will provide additional errors lower than +/- 3 saturation units, on the whole range of centrifuge geometries. These are SPL and Sαβ including radial correction and consistency constraints.

When the best solutions are used, with radial correction, consistency constraints and a proper numerical implementation, an error close to +/- 3 saturation units may be expected from the interpretation process whatever the centrifuge geometry.

## V CONCLUSIONS

The present survey demonstrated that :

1.) The main source of inaccuracy in the drainage capillary pressure curve determination by centrifuge is related to the interpretation process and not to experimental procedures (assuming accepted procedures are in use) nor to shape of the capillary pressure curve.

2.) The inaccuracy depends on the centrifuge geometry (and resulting contributions of centrifugal and radial effects) and on the method used for solving the centrifuge equation.

3.) Additional errors due to the inversion process may be very large (+/-10 saturation units). They **cannot** be reduced significantly by increasing the number of rotation steps or by reducing the experimental error below 2 saturation units or by averaging the results from different interpretation processes.

4.) The only way to improve the capillary pressure curve determination is to use an appropriate solution of the centrifuge equation, consistent with the centrifuge and core geometry.

5.) Whatever the geometry in use, only a few solutions may insure a reasonable accuracy, i.e. below +/- 3 saturation units. These are SPL and Sαβ.

6.) These solutions require a proper implementation and the use of correction for radial effects and (or) the use of consistency constraints.

7.) A figure is provided (Figure 12) to evaluate the additional errors due to the interpretation process for most of the other solutions in use in the industry (the experimental error, on average saturation measurements, has to be added to obtain the total error). Their accuracy is always improved by using radial correction or consistency constraints.

## ACKNOWLEDGEMENTS

The survey was performed thanks to the active participation of laboratories from different oil & gas companies, contractors or R&D institutes. Thanks are expressed to all of them for their contribution.

Jill Buckley and Andre Bouchard are thanked for their helpful comments and suggestions.

## NOMENCLATURE

Latin

r : Radial distance from the centrifuge axis to a point in the centrifuged core

$r_1$ : r at the inner core face

$r_3$ : r at the outer core face

Pc, P : Capillary pressure

Pd : Capillary Pressure threshold

$P_1$ : Pc evaluated at $r_1$

S :Wetting phase saturation

<S> : Average wetting phase saturation

B : Dimensionless factor related to the extend of the centrifugal shape of the pressure field (see text)

N : Dimensionless factor related to the extend of radial effect, i.e. the extend of the curvature of the pressure field (see text)

M :Dimensionless factor related to the extend of gravity effect, i.e. the extend of the gravity field versus the centrifuge field (see text)

x, y, z : Integration variables

$a_o$, $b_o$, b : Parameters (see text)

g : Gravitational constant

R : Radius of core

H, W, L : Error parameters (see text)

Greek

ρ : Phase mass density

ω : Centrifuge angular velocity

δ90 : Error parameter (see text

Metric units

Pc : pascal, Pa.

r : meter, m.

ρ : kilogram per cubic meter, $kg/m^3$.

ω : radian per second, rad/s.

Conversion factors:

Pc:

| from/to | m | cm | inch |
|---|---|---|---|
| m | 1 | $10^2$ | 39.37 |
| cm | $10^2$ | 1 | $3.937\ 10^{-1}$ |
| inch | $2.54\ 10^{-2}$ | 2.54 | 1 |

ω:

| from/to | $kg/m^3=g/l$ | pound per cubic inch |
|---|---|---|
| $kg/m^3=g/l$ | 1 | $3.6127\ 10^{-5}$ |
| pound per cubic inch | $2.7680\ 10^4$ | 1 |

r:

| from/to | mbar | bar | Pa | MPa | psi |
|---|---|---|---|---|---|
| mbar | 1 | $10^{-3}$ | $10^2$ | $10^{-4}$ | $1.45\ 10^{-2}$ |
| bar | $10^3$ | 1 | $10^5$ | $10^{-1}$ | 14.5037 |
| Pa | $10^{-2}$ | $10^{-5}$ | 1 | $10^{-6}$ | $1.45\ 10^{-4}$ |
| MPa | $10^4$ | 10 | $10^6$ | 1 | $1.45\ 10^2$ |
| psi | 68.94 | $6.894\ 10^{-2}$ | $6.894\ 10^3$ | $6.894\ 10^{-3}$ | 1 |

ρ:

| from/to | rad/s | RPM |
|---|---|---|
| rad/s | 1 | 9.549 |
| RPM | $1.04710^{-1}$ | 1 |

## REFERENCES


Anli J., 1973, An Investigation into the Functional Relationship between Capillary Pressure and Saturation in Porous Media, MSc Thesis, University of Alberta.

Andersen A.S, and White E.T., 1971, Improved Numerical Methods for Voltera Equations of the First Kind. The Computer J., V. 14, N. 4, p. 442-443.

Anderson, W.G, 1986, Wettability literature survey-Part 2, Wettability measurement. Journal of Petroleum Technology, Nov. 1986, p. 1246-1262.

Ayappa, K.G., Davis, H.T., Davis, E.A., and Gordon, J., 1989, Capillary pressure, centrifuge method revisited. AIChE Journal, V. 35, N 3, 365-372.

Ayappa, K.G., Abraham E.A., Davis, H.T., Davis, E.A., and Gordon, J., 1994, Influence of sample with on deducing capillary pressure curves with the centrifuge. Chemical Engineering Science, V. 39, N 3, p. 327-333.

Blackwell, R.J., 1991, Capillary Pressure Measurements of Heterogeneous Cores Using a Centrifuge, *SCA* paper *9105* presented (orally) at The Society of Core Analysts Annual Technical Conference, San Antonio, Texas, August 21-22.

Bentsen, R.G., and Anli, J., 1977, Using parameter estimation techniques to convert centrifuge data into capillary pressure curve. SPE Journal, p. 57-64.

van Domselaar, H.R., 1984, An exact equation to calculate actual saturations from centrifuge capillary pressure measurements. Rev. Tec. INTEVEP, V. 4, N. 1, p. 55-62.

Chen, Z. Liu, H.Q. and Yao, J, 1992, New Capillary Pressure Models for parameter estimation to interpret Centrifuge data. SPE paper 24045, SPE Western Regional Meeting, Bakersfield, CA, March 30-April 1.

Chen, Z.A. and D.W. Ruth, 1994, Centrifuge Capillary Pressure Data Interpretation : Gravity Degradation Aspect Consideration. SCA paper 9425, Society of Core Analysts conference, Stavanger, Sept. 12-14 1994, pp. 275-284.

Chen, Z.A. and D.W. Ruth, 1994, Gravity Degradation Effect on Low-Speed Centrifuge Capillary Pressure Data, accepted by *AIChE* Journal for publication, 1994.

Chen, Z.A. and D.W. Ruth, 1993, Centrifuge Capillary Pressure Reduction with Modified Forbes Method, Journal of Petroleum Science and Engineering, 9, 303-312.

Christiansen, R.L., 1992, Geometric Concerns for Accurate Measurement of Capillary Pressure Relationships with Centrifuge Methods, *SPE Formation Evaluation*, 7, 311-314.

Christiansen, R.L. and K.S. Cerise, 1987, Capillary Pressure: Reduction of Centrifuge Data, *paper 47d* presented at the 1987 AIChE Annual Meeting, New York City, Nov.15-20.

Clinch, S., 1995, Interpreting Centrifuge Capillary Pressure Data : the Approximation Solution. Centrifuge Notes, Personal communication, to be published.

Corey A.T., 1954, The Interelation between gas and oil relative permeabilities. Producers Monthly, Nov. p. 38-41.

Donaldson, E.C.,Thomas, R.D., and Lorenz, P.B.,1969, Wettability determination and its effects on recovery efficiency. SPE Journal March 1969, p.13-20.

Fleury M. and Forbes P.L., 1995 : Experimental évidence of radial effects on centrifuge capillary pressure curves. Proceedings of the SPWLA 36th Annual Logging Symposium, June 26-29, Paris,. Paper EE, 10p.

Forbes P.L., 1991 : Simple and accurate methods for converting centrifuge data into drainage and imbibition capillary pressure curves. 1991 Society of core analysts annual technical conference, August 20-22, San Antonio, paper 9107, 15p.

Forbes P.L., 1993 : Centrifuge determination of Capillary Pressure - Review of data analysis procedures. Workshop. SCA - 7th Annual Technical Conference of the Society of Core Analysts, Houston, Aug. 9-11, 1993, Proceedings.

Forbes P.L., 1994 : Simple and accurate methods for converting centrifuge data into drainage and imbibition capillary pressure curves. The Log Analyst, V. 35, N. 4, pp. 31-53

Forbes P.L., Chen Z. and Ruth D., 1994b : Quantitative Analysis Of Radial Effects On Centrifuge Capillary Pressure Curves", SPE paper 28182, SPE Fall meeting, New Orleans, Sept. 1994.

Forbes P.L., Ruth D. and Chen Z., 1994a : Dicussion of "Geometric Concerns For Accurate Measurement of Capillary Pressure Relationships With Centrifuge Method", SPE Formation Evaluation, March, pp. 79-80.

Forbes P.L. and Fleury M., 1995 : Radial effect and sample heterogeneity effect on Centrifuge capillary Pressure Curves. Proceedings of the International Symposium of the Society of Core Analysts, San Francisco, Sept. 12-14, 10 p.

Forbes P.L., 1997a : Quantitative Evaluation and Correction of Gravity Effects on Centrifuge Capillary Pressure Curves. Proceedings of the International Symposium of the Society of Core Analysts, Calgary September 8-10, 1997.

Forbes P.L., 1997b : Centrifuge Data Analysis Techniques : a SCA Survey on the Calculation of Drainage Capillary Pressure Curves from Centrifuge Measurements. A Report of the Society of Core Analysts.

Glotin, J., Genet, J., and Klein, P., 1990, Computation of drainage and imbibition capillary pressure curves from centrifuge experiments. SPE paper 20502, 1990 Annual Technical Conference and Exhibition, New Orleans, Sept. 23-26, p. 313-324.

Golaz P. and Bentsen R.G., 1980 : On the Use of the Centrifuge to Obtain Capillary Pressure Data. 31st Ann. Tech. Meet. Pet. Soc. CIM, Calgary, Alberta, May 25-28, paper 80, 31-88.

Hassler, G.L., and Brunner, E., 1945, Measurements of capillary pressure in small core samples,. Trans. AIME, 160, 114-123.

Hermansen, H., Eliassen, O., Guo, Y., and Skjaeveland, S.M., 1991, Capillary pressure from centrifuge- A new direct method. Advances in core evaluation II, Reservoir Appraisal, Worthington and Longeron eds., Gordon and Breach Science Publishers, (Reviewed Proceedings of the SCA Conference Eurocas II, London, UK, 20-22 Mai 1991), p. 453 - 468.

Hirasaki, G.J., O'Meara, D.J., and Rohan, J.A., 1988, Centrifuge measurements of capillary pressure, Part 2 - Cavitation, SPE paper 18592, Annual Technical Conference Houston.

Hirasaki, G.J. , Rohan, J.A., and Dubey, S.T., 1990, Wettability evaluation during restored state core analysis. SCA Conference paper 9016., Aug. 15-16, Dallas 1990, 30 p.

Hirasaki, G.J. and J.A. Rohan, 1993, Recommendations for Determining Production Data, presentation at The Centrifuge Capillary Pressure Workshop, The Society of Core Analysts Annual Technical Conference, Houston, Texas, August 9-11.

Hoffman, R.N., 1963, A technique for the determination of capillary pressure curves using a constantly accelerated centrifuge. Trans AIME, 228, p. 227-235.

Jaimes O., 1991, Centrifuge Capillary Pressure : Method of the Center of Forces, SPE paper 22687, Annual technical conference and exhibition, Dallas, October 6-9, 1991, pp. 293-303

King, M.J., Narayanan, K.R., and Falzone, A.J., 1990, Advances in centrifuge methodology for core analysis. 1990 SCA Conference, Paper 9011, , Aug. 15-16, Dallas 1990 24 p.

King, M.J., Falzone, A.J., Cook W.R., Jennings, J.W. jr. and Mills W.H., 1986, Simultaneous Determination of Residual Saturation and Capillary Pressure Curves Utilizing the Ultracentrifuge. *SPE paper 15595* presented at The 61th SPE Annual Technical Conference and Exhibition, New Orleans, Oct. 5-8.

Kolltveit K., Nordtvedt J.E., Nordaas K. and Watson A.T., 1996, Estimation of Capillary Pressure Functions From Centrifuge Data, Proceedings of the second International Conference on Inverse Problems in Engineering : Theory and Practice, 9-14 June 1996, Le Croisic, France, 9 p.

Luffel D. L., 1964, Discussion on Hofman's Paper, SPE Journal, p. 191.

Melrose, J.C., 1988, Interpretation of the Centrifuge Capillary Pressure data : the Log Analyst, V 29, N1, pp. 40-47.

Melrose, J.C., 1990, Valid Capillary pressure data at low wetting phase saturations, SPE Reservoir Engineering, February 1990, pp. 95-99.

Nordtvedt, J.E., 1989, Using the Inverse Problem Formulation to Calculate Characteristic Properties of the Porous Medium. PhD Thesis, Bergen University, Norway.

Nordtvedt, J.E., and Kolltveit, K., 1991, Capillary pressure curves from centrifuge data by use of spline functions, SPE Reservoir Engeering paper, November 1991, pp. 497-501..

Nordtvedt, J.E., Watson A.T., Mejia, G., and, Yang, P., 1990, Estimation of capillary pressure and relative permeability functions From centrifuge experiments. SPE unsolicited paper 20805.

O'Meara,D.J., Hirasaki, G.J., and Rohan, J.A., 1988, Centrifuge measurements of capillary pressure, Part 1-Outflow boundary condition. SPE paper 18296, Annual Technical Conference Houston.

O'Meara,D.J., Hirasaki, G.J., and Rohan, J.A., 1992, Centrifuge measurements of capillary pressure, Part 1-Outflow boundary condition. SPE Reservoir Engineering, p. 133-142.

Rajan, R.R., 1986, Theoretically correct analytical solution for calculating capillary pressure-saturation from centifuge experiments. SPWLA Annual Logging Symp., June 9-13, p. 1-17.

Ruth, D., and Wong, S., 1988, Calculation of capillary pressure curves from data obtained by the centrifuge method. 1988 SCA Conference, Aug 17-18, paper 8802, 9 p.

Ruth, D., and Wong, S., 1990, Centrifuge capillary pressure curves. Journal of Canadian Petroleum Technology, v. 29, N. 3, p. 67-72.

Ruth, D., and Wong, S., 1991, Calculation of capillary pressure curves from data obtained by the centrifuge method. The Log Analyst, v. 32, n. 5, p. 575-582.

Ruth, D., and Chen Z.A., 1995, On the measurement and interpretation of centrifuge capillary pressure curves. The SCA survey data. The Log Analyst, v. 36, n. 5, p. 21-33.

Sabatier L., 1994, Comparative Study of Drainage Capillary Pressure Measurements using Different Techniques and for Different Fluid Systems, SCA paper 9424, Society of Core Analysts conference, Stavanger, Sept. 12-14, 1994, pp. 263-273

SCA, 1993, Capillary Pressure Determination Using The Centrifuge,Workshop. SCA - 7th Annual Technical Conference of the Society of Core Analysts, Houston, Aug. 9-11, 1993, Proceedings.

Skuse, B., Firoozabadi, A., and Ramey, H.J., 1988, Computation and interpretation of capillary pressure from a centrifuge. SPE paper 18297, Annual Technical Conference,Houston, Octb. 2-5, p..

Slobod, R.L., Chambers, A., and Prehn, W.L., 1951, Use of centrifuge for determinig connate water, residual oil, and capillary presusre curves of small core samples. Pet. Transac. AIME, 192, p. 127-134.

Thomeer, J.H.M., 1960, Introduction of a pore geometrical factor defined by the capillary pressure curves. Petroleum Transaction, AIME, N. 219, p. 354-358.

Ward J.S. and Morrow N.R., 1985, Capillary pressure and gas relative Permeabilities of low permeability sandstones, SPE/DOE 13882, SPE/DOE conference on low permeability gas reservoirs, Denver, Colorado, May 19-22, 1985.

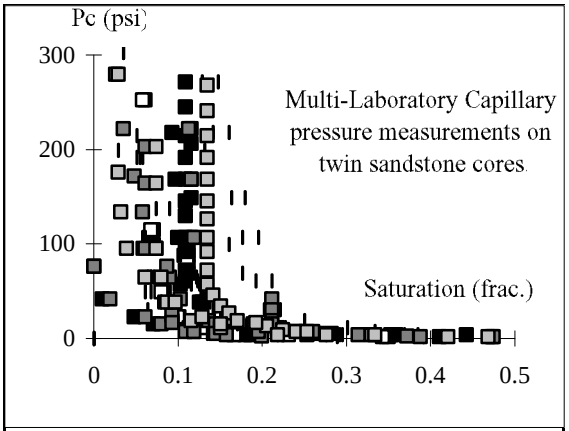


Figure 1 : Variability of results in the first SCA survey on drainage centrifuge capillary pressure curves.

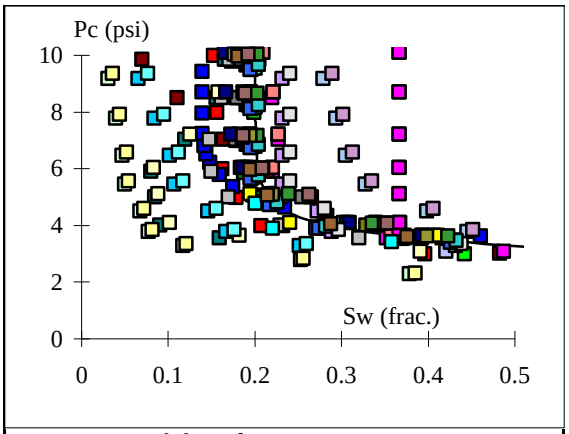


Figure 5 : Variability of interpretations provided by the different laboratories. Case 2.

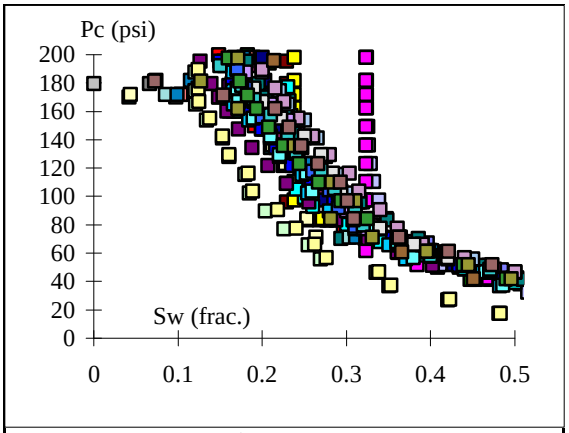


Figure 6 : Variability of interpretations provided by the different laboratories. Case 7.

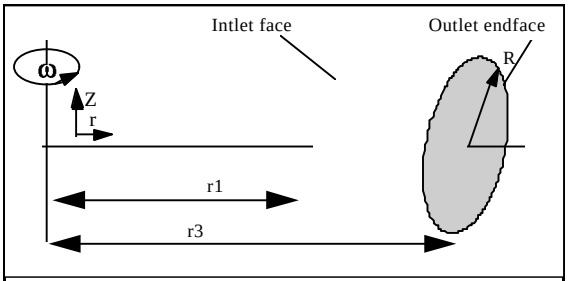


Figure 2 : The Centrifuge geometry. Core samples are rotated around a vertical axis.

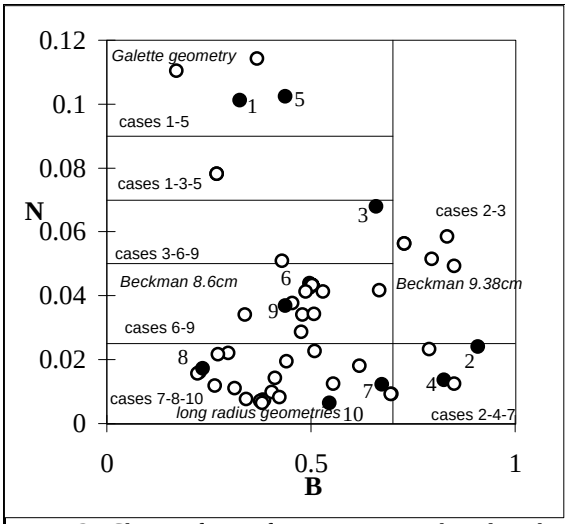


Figure 3 : Choice of centrifuge geometry. White dots show litterature data. Black dots are the survey geometries.

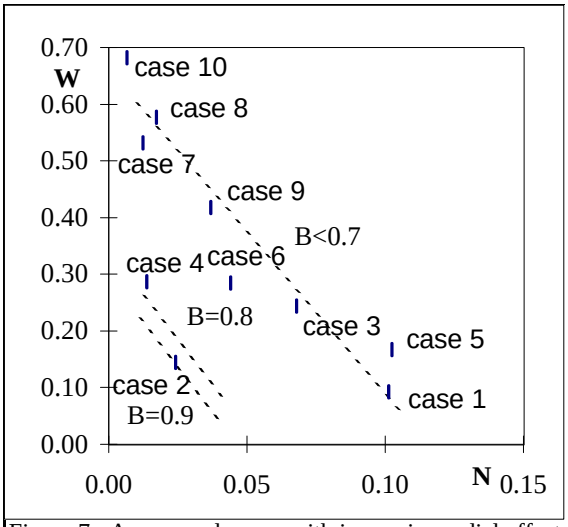


Figure 7 : Accuracy damage with increasing radial effect (N).

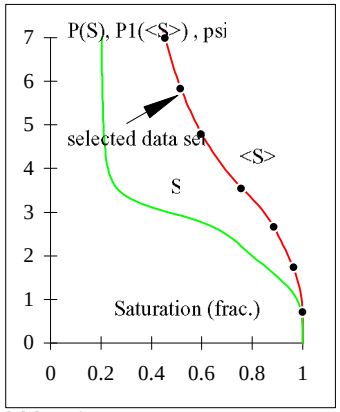


**CASE N° 1**

| | | |
|---|---|---|
| Core Len RPM | 2.5 | cm. |
| Core diameter | 5.08 | cm. |
| Core porosity | 20 | % |
| Bottom radius (oulet) | 14 | cm. |
| Error on rotation speed | 10 | RPM. |
| Error on production volu | 0.03 | cm3 |
| Brine density | 1.036 | kg./l. |
| Oil/air density | 0.8 | kg./l. |

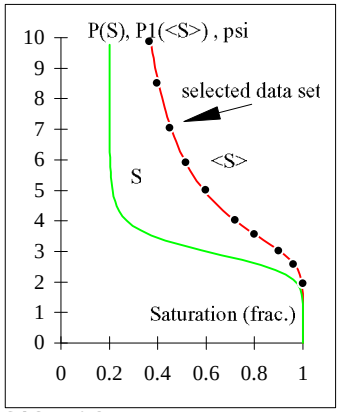


**CASE N° 2**

| | | |
|---|---|---|
| Core Length | 6 | cm. |
| Core diameter | 2.54 | cm. |
| Core porosity | 25 | % |
| Bottom radius (oulet) | 8.6 | cm. |
| Error on rotation speed | 10 | RPM. |
| Error on production volu | 0.05 | cm3 |
| Brine density | 1.036 | kg./l. |
| Oil/air density | 0.8 | kg./l. |

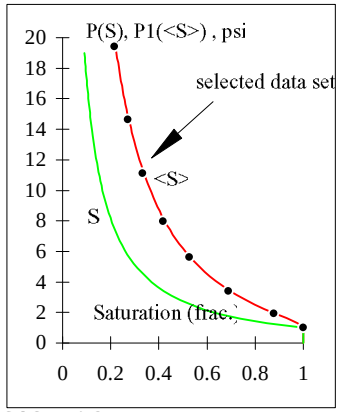


**CASE N° 3**

| | | |
|---|---|---|
| Core Length | 5 | cm. |
| Core diameter | 5.08 | cm. |
| Core porosity | 10 | % |
| Bottom radius (oulet) | 12 | cm. |
| Error on rotation speed | 10 | RPM. |
| Error on production volu | 0.08 | cm3 |
| Brine density | 1.036 | kg./l. |
| Oil/air density | 0.8 | kg./l. |

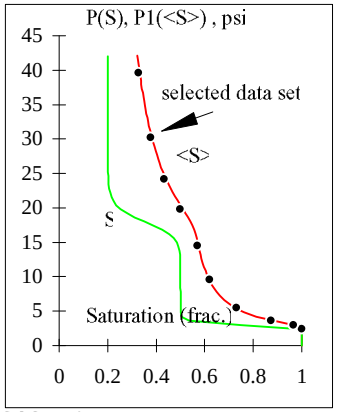


**CASE N° 4**

| | | |
|---|---|---|
| Core Length | 7 | cm. |
| Core diameter | 2.54 | cm. |
| Core porosity | 22 | % |
| Bottom radius (oulet) | 12 | cm. |
| Error on rotation speed | 10 | RPM. |
| Error on production volu | 0.09 | cm3 |
| Brine density | 1.036 | kg./l. |
| Oil/air density | 0.8 | kg./l. |

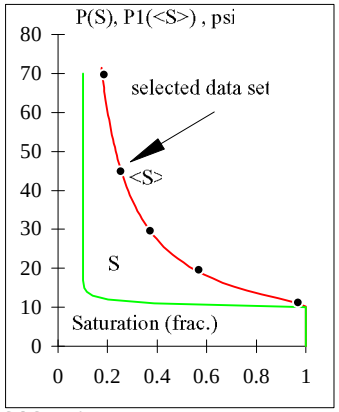


**CASE N° 5**

| | | |
|---|---|---|
| Core Length | 1.5 | cm. |
| Core diameter | 2.54 | cm. |
| Core porosity | 22 | % |
| Bottom radius (oulet) | 6 | cm. |
| Error on rotation speed | 10 | RPM. |
| Error on production volu | 0.02 | cm3 |
| Brine density | 1.036 | kg./l. |
| Oil/air density | 0 | kg./l. |

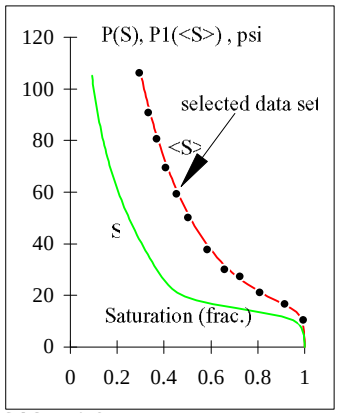


**CASE N° 6**

| | | |
|---|---|---|
| Core Length | 2.5 | cm. |
| Core diameter | 2.54 | cm. |
| Core porosity | 16 | % |
| Bottom radius (oulet) | 8.6 | cm. |
| Error on rotation speed | 10 | RPM. |
| Error on production volu | 0.03 | cm3 |
| Brine density | 1.036 | kg./l. |
| Oil/air density | 0 | kg./l. |

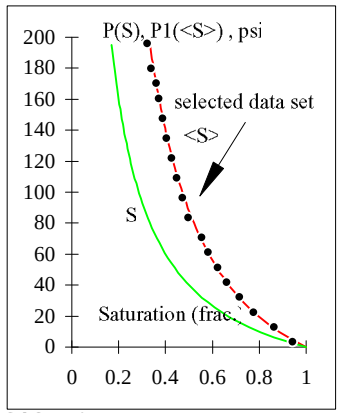


**CASE N° 7**

| | | |
|---|---|---|
| Core Length | 6 | cm. |
| Core diameter | 2.54 | cm. |
| Core porosity | 14 | % |
| Bottom radius (oulet) | 14 | cm. |
| Error on rotation speed | 10 | RPM. |
| Error on production volu | 0.07 | cm3 |
| Brine density | 1.036 | kg./l. |
| Oil/air density | 0 | kg./l. |

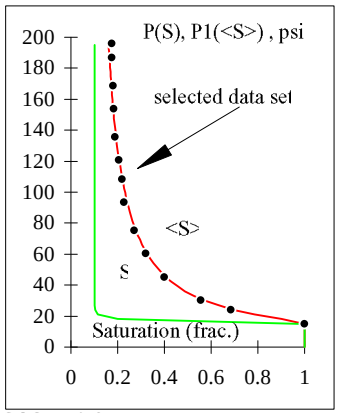


**CASE N° 8**

| | | |
|---|---|---|
| Core Length | 2.5 | cm. |
| Core diameter | 2.54 | cm. |
| Core porosity | 18 | % |
| Bottom radius (oulet) | 20 | cm. |
| Error on rotation speed | 10 | RPM. |
| Error on production volu | 0.04 | cm3 |
| Brine density | 1.036 | kg./l. |
| Oil/air density | 0 | kg./l. |

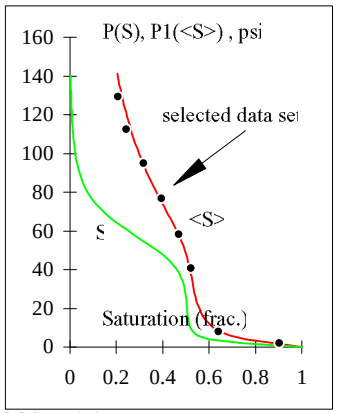


**CASE N° 9**

| | | |
|---|---|---|
| Core Length | 2.5 | cm. |
| Core diameter | 2.54 | cm. |
| Core porosity | 25 | % |
| Bottom radius (oulet) | 10 | cm. |
| Error on rotation speed | 10 | RPM. |
| Error on production volu | 0.06 | cm3 |
| Brine density | 1.036 | kg./l. |
| Oil/air density | 0 | kg./l. |

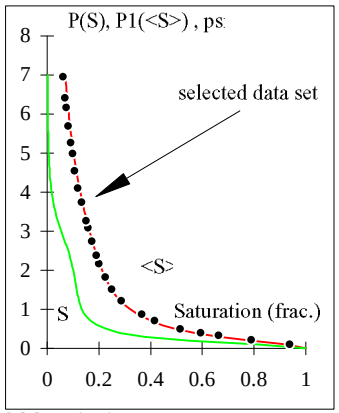


**CASE N° 10**

| | | |
|---|---|---|
| Core Length | 7 | cm. |
| Core diameter | 2.54 | cm. |
| Core porosity | 12 | % |
| Bottom radius (oulet) | 21.5 | cm. |
| Error on rotation speed | 10 | RPM. |
| Error on production volu | 0.1 | cm3 |
| Brine density | 1.036 | kg./l. |
| Oil/air density | 0.8 | kg./l. |

**Figure 4 :** Selected Artificial Data and related Capillary Pressure Curves (S). <S> is the exact measurement calculated including radial and gravity effects. Artificial data (black dots) have been obtained by sampling on the <S> curves and including error in rotation speed and production volume measuremen

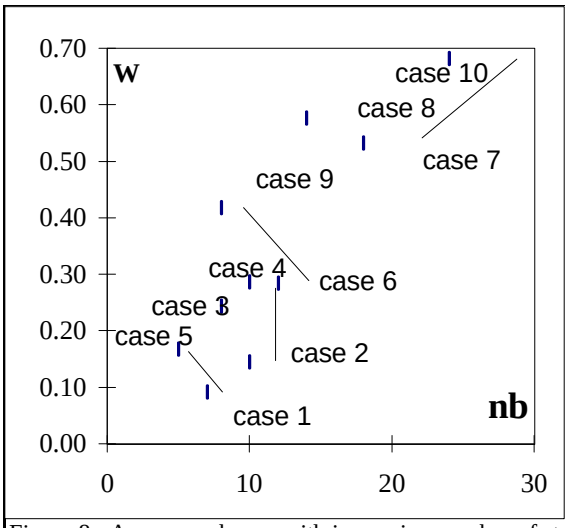


Figure 8 : Accuracy change with increasing number of step of measurement. Lines connect cases to be compared, i.e. with similar B and N values.

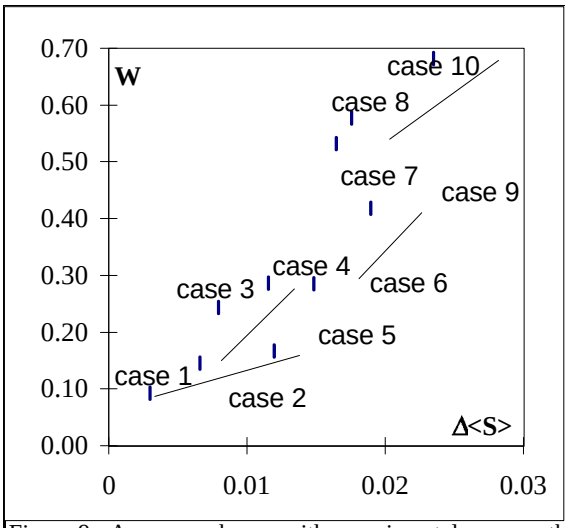


Figure 9 : Accuracy change with experimental error on the average saturation measurement, Δ<S>. Lines connect cases to be compared, i.e. with similar B and N values.

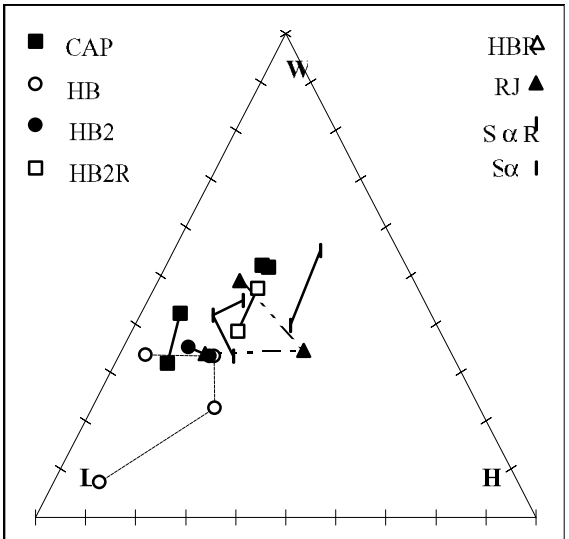


Figure 10 : LWH diagram for identical solutions with different numerical implementation ( algorithms, constraint, smoothing, ....).

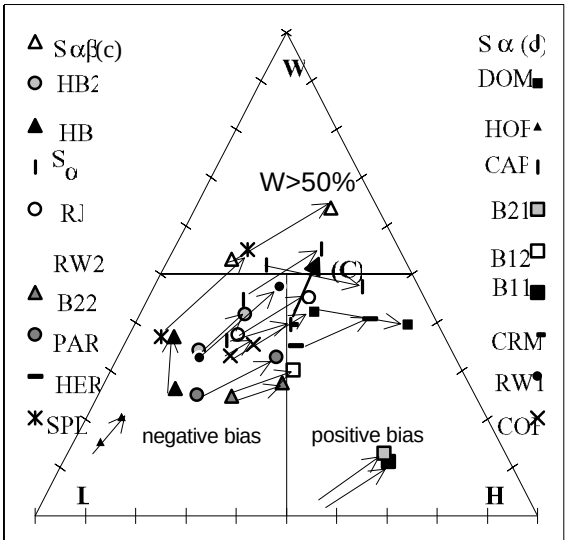


Figure 11 : LWH diagram for the interpretation methods. Arrows indicate the effect of radial correction.
(C) shows the effect of using consistency constraints.

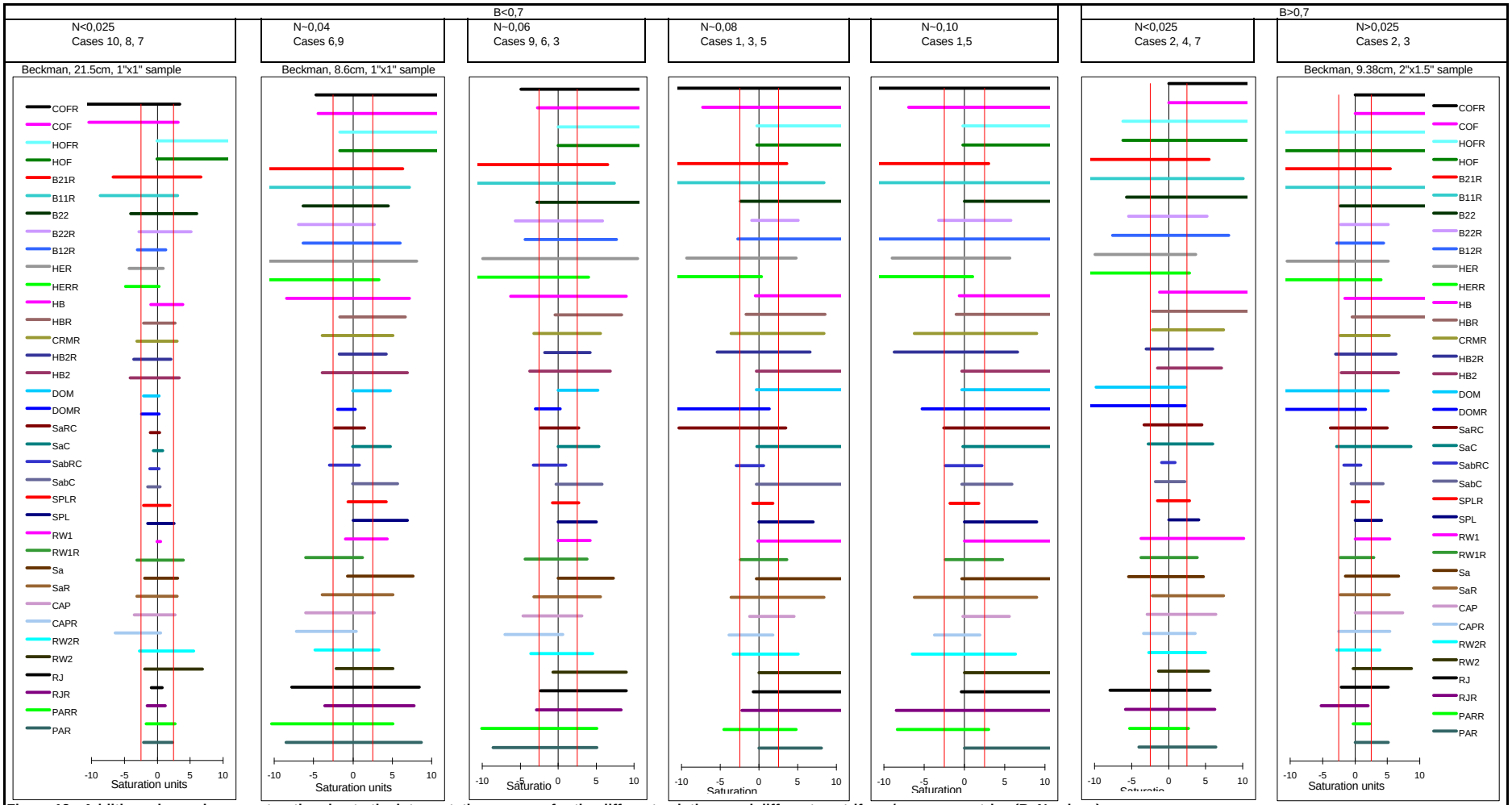


**Figure 12 : Additionnal error bar on saturation due to the interpretation process for the different solutions and different centrifuge / core geometries (B, N values).**
**Total error bar is obtained by adding the experimental error bar on average saturation measurement, +/-Δ<S>. Error on rotation speed measurement is assumed to be low, 10 RPM.**